Rock Mechanics
and Rock Engineering 18, 267—292 (1985)

**Rock Mechanics
and Rock Engineering**

Progressive Failure in Stratified and Jointed Rock Mass

By

Mustafa Gencer

Visiting Scientist, Massachusetts Institute of Technology, U. S. A.

Summary

This paper describes a mathematical model for analyzing progressive failure in a stratified and jointed rock mass dipping parallel to the slope face. The relationship between the necessary support forces and permissible displacement in the rock mass is discussed. An analytical expression is provided for the minimum required support force corresponding to a critical displacement. This expression is used to evaluate the potential of unstable failure propagation. The effect of time on progressive failure is considered by using a simple rheological model for joints. A case study, involving an excavation in a stratified medium, is used to compare model prediction with monitored performance.

1. Introduction

Sliding of stratified and jointed rock is often accompanied by internal deformation leading to a non uniform shear stress distribution along the discontinuity planes, which causes the development of progressive failure. Once strain softening behavior of overconsolidated clays became known, it was a logical extension to consider the mechanism of progressive failure in stability analysis of earth and rock slopes (Skempton, 1964; Bishop, 1967; Müller, 1966). Probably, the first and most complete description of progressive failure has been given by Bjerrum (1967) for overconsolidated clay shales sliding along surfaces striking parallel to the slope. This was followed by successful approaches to analyze the mechanism as described by Bjerrum (Müller and Malina, 1968; Christian and Whitman, 1969; Suklje, 1971; Palmer and Rice, 1973). However, these studies are based on some restrictive hypotheses and do not take into account the dependency between permissible displacements on the one hand and the required support forces on the other hand. This interaction is considered by Descoeudres and Gencer (1979) employing a numerical approach and physical model tests.

This paper constitutes an extension of this earlier work (see also Gencer, 1982). The interaction between the required support forces and displacements is discussed. An analytical expression is given for the minimum required support force. It will also be shown how this minimum

force can be used to evaluate the unstable propagation of failure in a stratified rock mass dipping parallel to the slope face.

The mathematical model is verified by applying it to an actual excavation and comparing observed and analytically predicted displacements.

2. Mechanism of Progressive Failure

A stratified and jointed rock mass is shown in Fig. 1. It is assumed that an excavation is made down to the depth H and that failure occurs along the bedding plane passing through the base of the excavation. Accord-

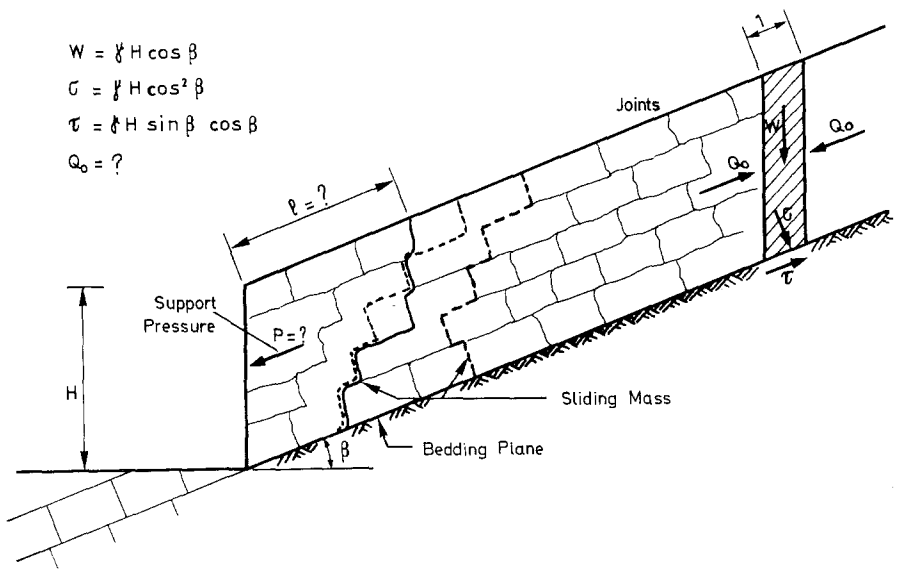

Fig. 1. A stratified and jointed rock mass dipping parallel to the slope surface, initial equilibrium and possible shapes of the sliding mass after excavation

ing to Rankine's hypothesis the stability of the slope can be defined by considering the equilibrium of a unit slice (Fig. 1). Initially the only shear stress existing along the bedding plane is that due to gravity

$$\tau = \gamma H \sin \beta \cos \beta \tag{1}$$

where γ is the unit weight and the other parameters as shown in Fig. 1. It is assumed that the slope is stable before excavation and τ is smaller than peak shear strength. The lateral forces Q_0 acting at both sides of the slice are equal and opposite, they are thus uniformly distributed inside the rock mass. This force represents, e. g., the lateral stresses remaining in a over-consolidated soil mass after the removal of the overburden pressure by erosion. In the case of rock slopes, Q_0 is related to the global influence of geological history (action of tectonic forces, overburden pressure of glaciers,

overconsolidation of sedimentary rocks). An excavation will affect a relatively small zone within the rock mass compared to its geological dimensions. Thus for practical purposes, the uniform distribution of Q_0 in that zone before excavation is a reasonable assumption. Uniform distribution of Q_0 means it does not affect the equilibrium of the individual slice; therefore stability can only exist if the driving force (i. e. mobilized shearing resistance) is smaller than peak shear strength. This justifies the assumption made above.

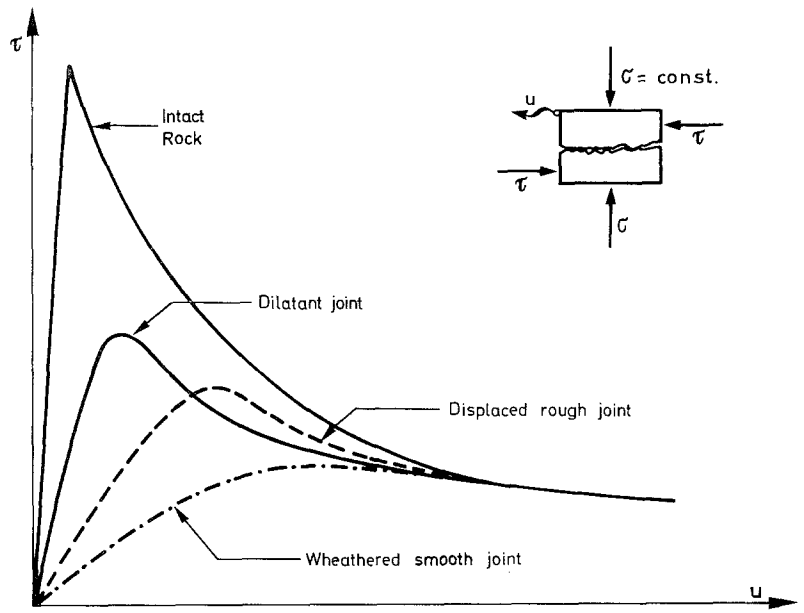

Fig. 2. Variation of the shearing resistance with displacements for rough rock joints

The removal of this lateral support force Q_0 by the excavation will cause a redistribution of the stresses inside the rock mass. The failure is initiated somewhere along the bedding plane where shear stresses exceed the peak shear strength. This lateral unloading will cause the rock mass to move towards the excavation by sliding along the bedding plane. Since rough joints and some filled joints typically follow a strain-softening behaviour (as shown in Fig. 2), increasing displacements will lead to a reduction of shearing resistance from peak to residual. Therefore failure will progress along the bedding plane up to a point where the mobilized shear stresses are less than the shearing resistance.

The initiation and progression of failure will depend on the magnitude of the lateral force Q_0, on the lateral deformability due to the cross joints and most significantly on the shear stress-displacement behaviour of slope parallel joints (parallel to sliding plane). As pointed out by Bjerrum (1967) the rate of decay of the shear strength and the value of residual shear strength with respect to the initial shear stress τ due to the gravity, play a

very important role in the progression of failure. If the residual shear strength τ_r is greater than $\tau = \gamma H \cos\beta \sin\beta$ (the dip angle of the bedding plane is less then the residual friction angle) the failure will stop at a certain distance from the face of excavation when the removed natural force Q_0 is entirely redistributed along the bedding plane.

On the other hand if τ_r is less than τ (the dip is greater than the residual friction angle), a given size of rock block will continue to slide downhill under the effect of the gravity. This will cause the reduction of the natural force Q_0 at a certain distance from the excavation face. Failure is initiated again at this point and the size of sliding block will increase continuously. This unstable progression of failure may be prevented by replacing the removed force Q_0 with a relatively modest support force before the excessive displacements occur in the rock mass (Descoeudres, 1974).

3. Mathematical Model for Progressive Failure

The simplified geometry of a layer in a stratified rock mass dipping parallel to the slope surface which will be considered in the analysis is shown in Fig. 3a. The layer is divided into identical individual blocks (the weight W is the same for all blocks) by a set of cross joints and the lateral force Q_0 acts perpendicularly to the cross joints, as mentioned before.

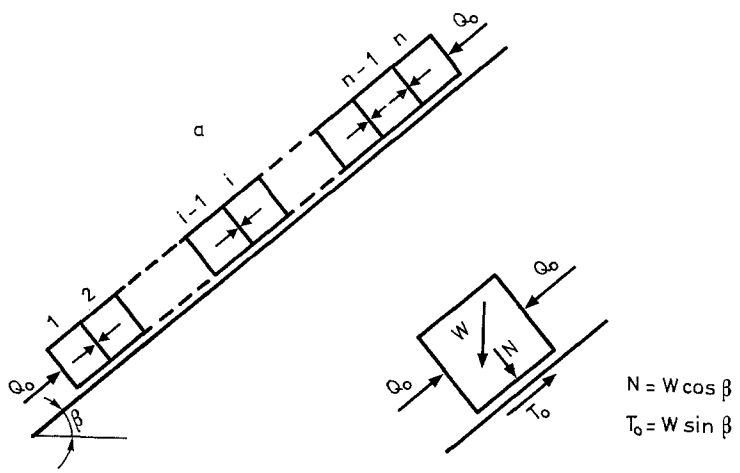

Fig. 3. Simplified geometry of the rock mass
a) Initial distribution of the forces

Before excavation each block is in equilibrium without displacement, i. e., the forces Q_i between blocks are all equal to Q_0, and the component of gravity weight parallel to bedding plane is compensated by the shearing resistance T_0 mobilized on the bedding plane (Fig. 3a):

$$T_0 = W \sin\beta. \tag{2}$$

It is assumed that T_0 is less than the available peak shear strength on the bedding plane. Each block is then initially stable.

The excavation is simulated either by gradually reducing the initial force, i. e., a support force Q_1 less then Q_0 is applied (Fig. 3b) on the first block or by imposing a progressively increased displacement u_1 to the same

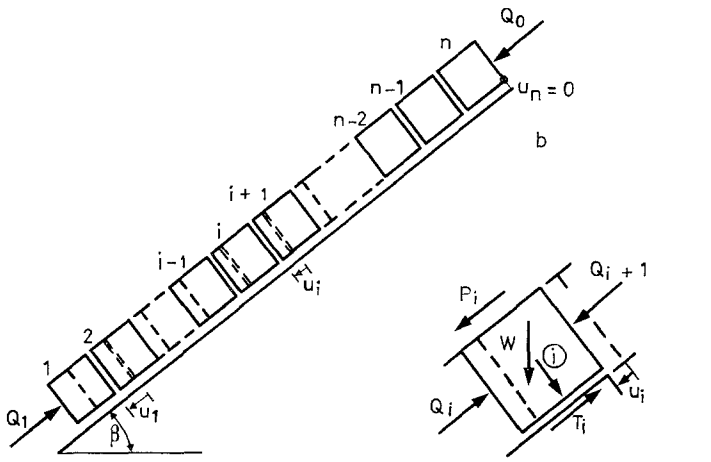

Fig. 3 b) Distribution of the forces after excavation

Fig. 3 c) Equilibrium of a single block

block. In both cases a new distribution of displacements and forces occurs within the layer. As Q_1 in further reduced (or u_1 increased) the number of blocks affected by this operation increases.

Different force-displacements relationships describing the behaviour of joints can be taken into account. The simplest relation between Q_i and displacements is linear (Fig. 4a).

$$Q_i = Q_0 - K_n\,(u_i - u_{i-1}) \tag{3}$$

u_i, u_{i-1} are displacements of neighbouring blocks, K_n is the normal stiffness of cross joints. A bilinear relation with two different normal stiffnesses K_n, K_n' or a hyperbolic relation with variable stiffness as defined by Goodman (1974) can also be used in the model (Fig. 4a).

The variation of the shear force with displacement for each block is shown in Fig. 4b. Four parameters are necessary to describe the complete behaviour; T_p and T_r are respectively peak and residual shear strength, K_s and K_s^* are shear stiffnesses.

$$\begin{aligned} &u_i < u_p && T_i = T_0 + K_s\,u_i \\ &u_p < u_i < u_r && T_i = T_p - K_s^*\,(u_i - u_p) \\ &u_i > u_r && T_i = T_r \end{aligned} \tag{4}$$

u_p and u_r represent the displacements corresponding to peak and residual shear strength.

The algorithm representing the motion of blocks is similar to the approach developed by Cundall (1971), relying on dynamic relaxation, which will be briefly explained:

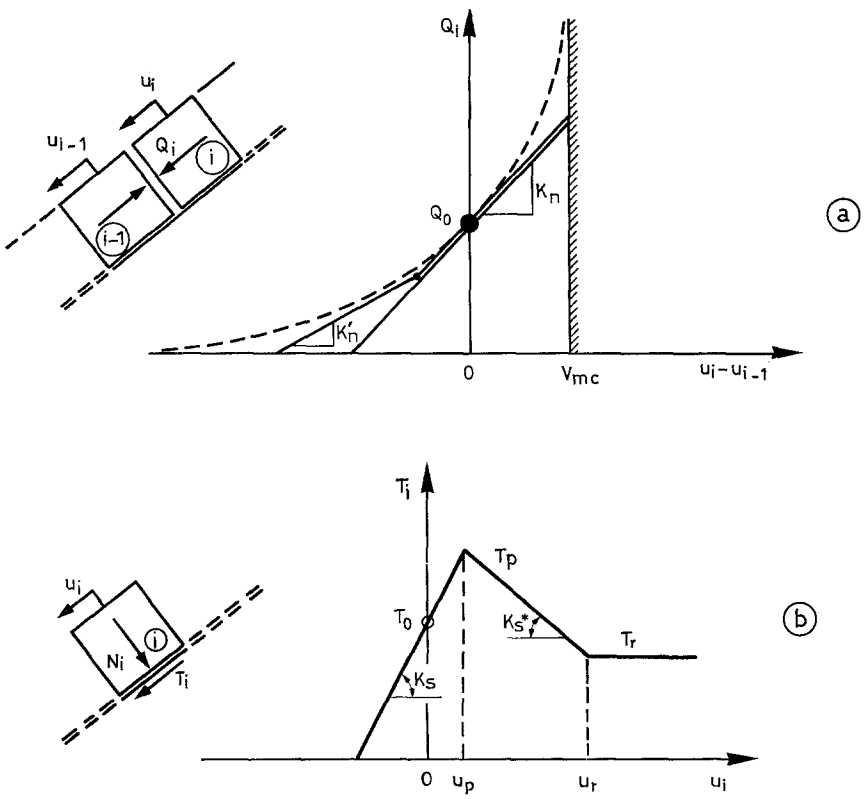

Fig. 4. Force-displacement relationships of joints
a) normal deformability; b) shearing behaviour

The forces acting on a block i are shown in Fig. 3c. These forces vary with displacements according to the relations defined above. The resultant force P_i is obtained from the equilibrium of the block.

$$P_i = Q_{i+1} - Q_i + W \sin \beta - T_i \tag{5}$$

The equation of motion for a block is given by the second law of Newton:

$$p_i = m \frac{d^2 u_i}{dt^2} \tag{6}$$

where m is the mass of a block, t represents the time.

Since a dynamic equation is used, the blocks will be continuously moving under the effect of the resultant force. The oscillations will occur due to the kinetic energy being developed in the block system. In order to ensure the convergence of displacements to a steady value equal to that of the static equilibrium an additional damping force R_i, acting on each block opposite to P_i, is introduced. The equation of motion is written as follows:

$$P_i - R_i = m \frac{d^2 u_i}{dt^2} \tag{7}$$

where

$$R_i = k\, v_i \tag{8}$$

k is a damping constant and v_i is the velocity of a block. The physical analogy of the model may be illustrated as follows: Assume that P_i represents a spring force which varies with displacements

$$P_i = -s\, u_i \tag{9}$$

s is a equivalent spring constant corresponding to the global stiffness of a block. The Eq. (7) becomes the equation of motion of a parallel spring dashpot system

$$m \frac{d^2 u_i}{dt^2} + k \frac{du_i}{dt} + s u_i = 0. \tag{10}$$

The damping constant considered here is an artifical one. The goal is to reach a static equilibrium state where the velocities, the forces P_i, R_i are equal to "zero" for all blocks. The integration of the equation of motion with respect to time is accomplished in time iteration steps (see Appendix). This is called dynamic relaxation, a numerical procedure to solve static problems with dynamic equilibrium equations (Otter et al., 1966) is used.

4. Interpretation of the Results

Characteristic curves as used in the analysis of underground openings are used to present the results. The variation of the force Q_1 which is required for equilibrium is related to the displacement of the first block. A typical result is shown in Fig. 5. Two principal cases (curves 1 and 2 in Fig. 5) can be distinguished:

Case 1: The residual shear strength T_r is higher than $T_0 = W \sin \beta$ (curve 1). The necessary support force vanishes after a certain amount of displacement u_x. In other words the progression of failure is stopped when the natural force Q_0 is completely distributed in the layer and taken up by shearing resistance along the bedding plane. This case will not be further pursued since it is inherently stable. Nevertheless the displacements may be of interest.

Case 2: Instability may occur if T_r is less than T_0 (Curve 2). Three different zones in the $Q_1 - u_1$ diagram (Fig. 5) have to be considered:

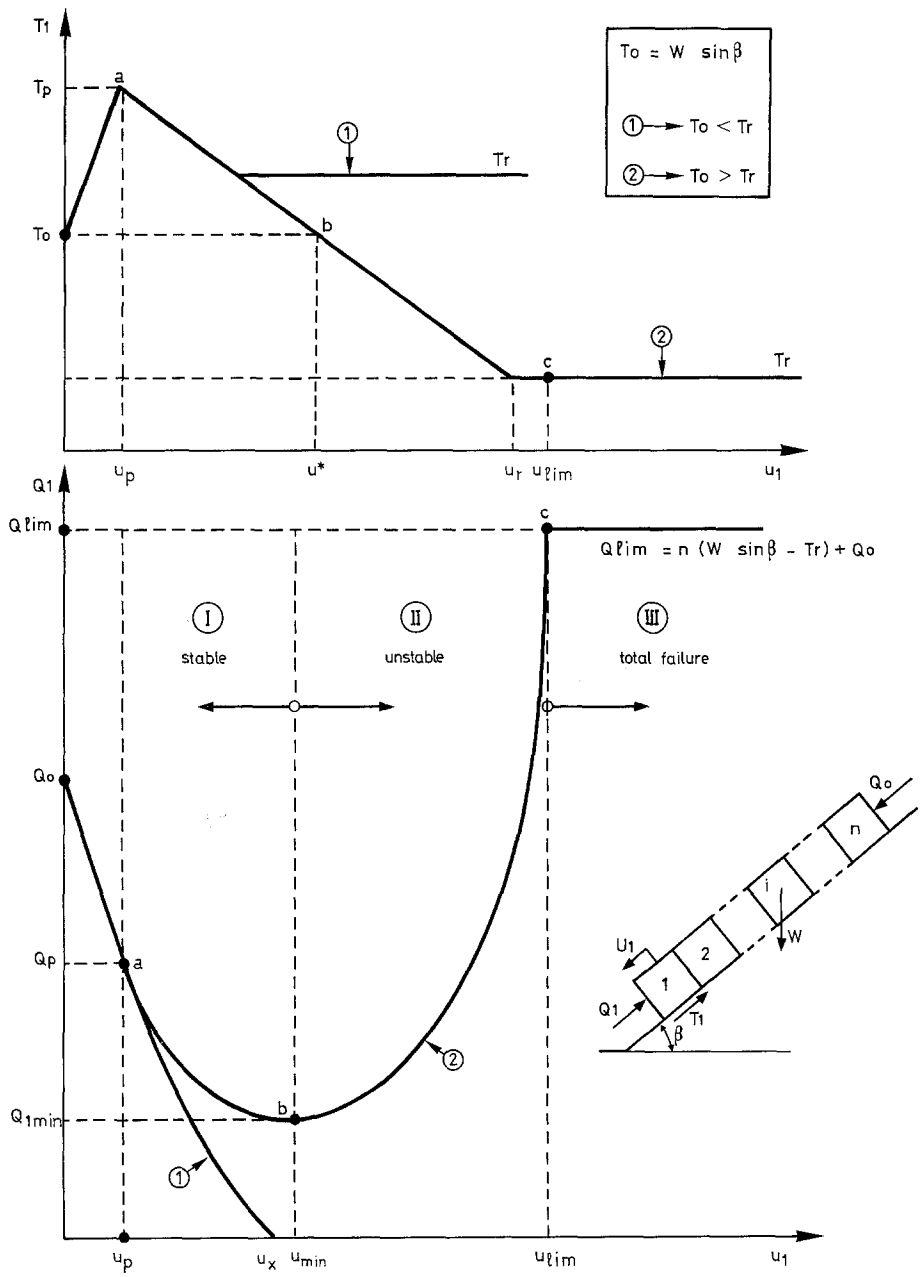

Fig. 5. Typical curves "support force Q_1-displacement" for different shearing resistance-displacement behaviour of the bedding plane

(a) The necessary support force decreases with displacements towards a minimum value $Q_{1\min}$ corresponding to an optimal mobilization of the shearing resistance along the bedding plane. The displacement at Q_1 is the critical displacement $u_{1\min}$. Propagation of failure is stable up to this point.

(b) The support force increases more or less rapidly with increasing displacements depending on the post peak behaviour of the bedding plane shearing resistance. In this domain the propagation of failure becomes unstable but it is still possible to stop it by increasing the required support force.

(c) The displacement reaches a limit value denoted by $u_{\lim}$ where a generalized failure occurs in the layer. The residual shear strength is mobilized everywhere and the final support force $Q_{\lim}$ depends on the length of layer, i. e., on the number n of blocks.

$$Q_{\lim} = Q_0 + n\,(W \sin\beta - T_r) \tag{6}$$

Physical model tests have been carried out by Descoeudres and Gencer (1979) to simulate progressive failure. The experimental support force displacement relationships are similar to those computed with the numerical model and shown in Fig. 5 (see Descoeudres and Gencer, 1979, Fig. 12). The existence of a minimum of support force and a limit displacement causing the failure of the entire layer was verified with these physical model tests.

Parametric studies were conducted on a large number of cases in which K_n, K_s, K_s^*, T_p, T_r and the force Q_0 were varied, typical results are shown in Fig. 6 from which the following conclusions can be drawn:

Unstable propagation of failure does not always occur even if the residual shear strength T_r is less than T_0. This depends on the combination of parameters introduced in the analysis.

Specifically:

1. The progression of failure is accompanied by differential displacements between blocks. They must be sufficiently large (low values of K_n) to make the mobilization of peak shear displacement possible when the initial normal forces between blocks are reduced.
2. The potential of unstable failure propagation will increase with ratio Q_0/T_p. The individual influence of Q_0 and T_p is shown in Fig. 6e and f. As expected unstable failure propagation does not occur for low values of Q_0 and high values of T_p. Thus, there is no failure for the extreme case $T_p = \infty$ (elastic shear behaviour Curve 1 in Fig. 6d) or relatively high T_p (curve 3 in Fig. 6e).
3. The potential for unstable failure propagation also increases with rapid decay of shear strength (high values of K_s^*, as illustrated by curves 3 and 4 in Fig. 6c). If K_s^* decreases the shape of shear strength-displacement relations tends toward curve 2 in Fig. 6d representing a stable case ($T_p = T_r$ and $K_s^* = 0$).

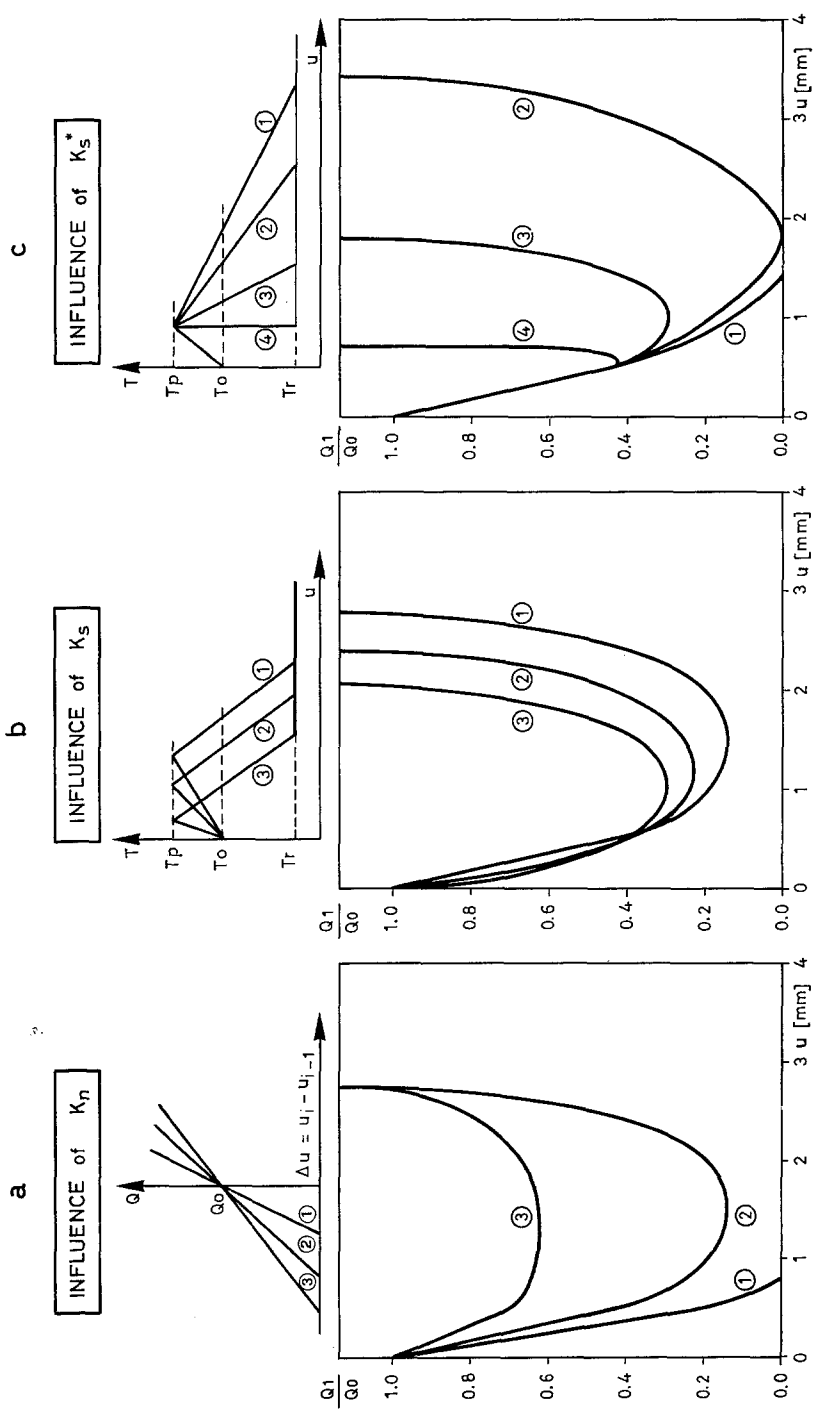

Fig. 6. Parametric studies. Influence of joint properties and Q_0 on support force-displacement relationships

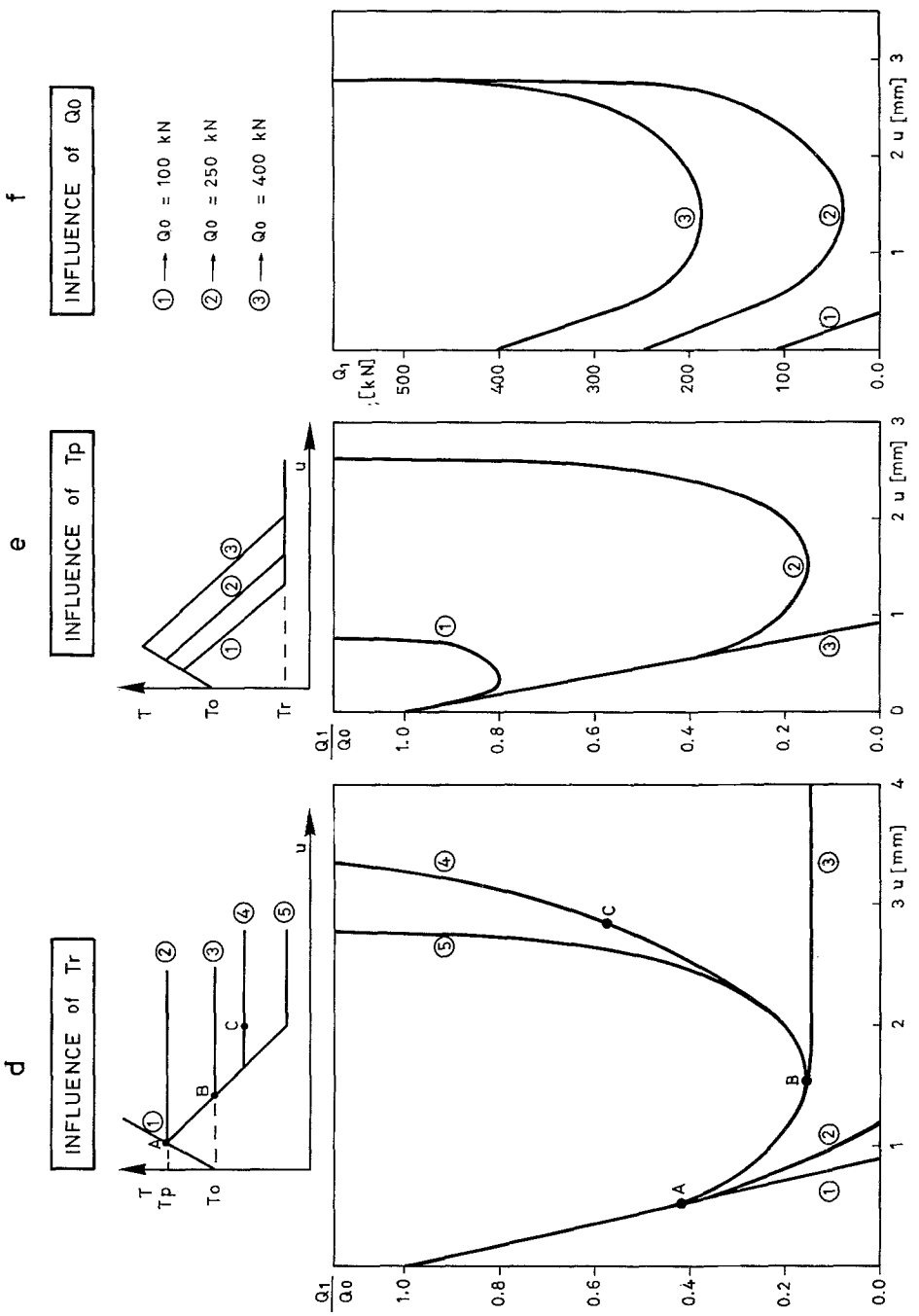
d
INFLUENCE of Tr
T
Tp
To
A
B
C
u
Q1/Q0
1.0
0.8
0.6
0.4
0.2
0.0
3 u [mm] 4
e
INFLUENCE of Tp
T
To
Tr
u
Q1/Q0
2 u [mm] 3
f
INFLUENCE of Q0
① → Q0 = 100 kN
② → Q0 = 250 kN
③ → Q0 = 400 kN
Q1 [kN]
500
400
300
200
100
0.0
2 u [mm] 3

The progression of failure in the layer is illustrated in Fig. 7. The distribution of the shear forces and displacement is shown for three different levels of displacements imposed on the first block; the displacements cor-

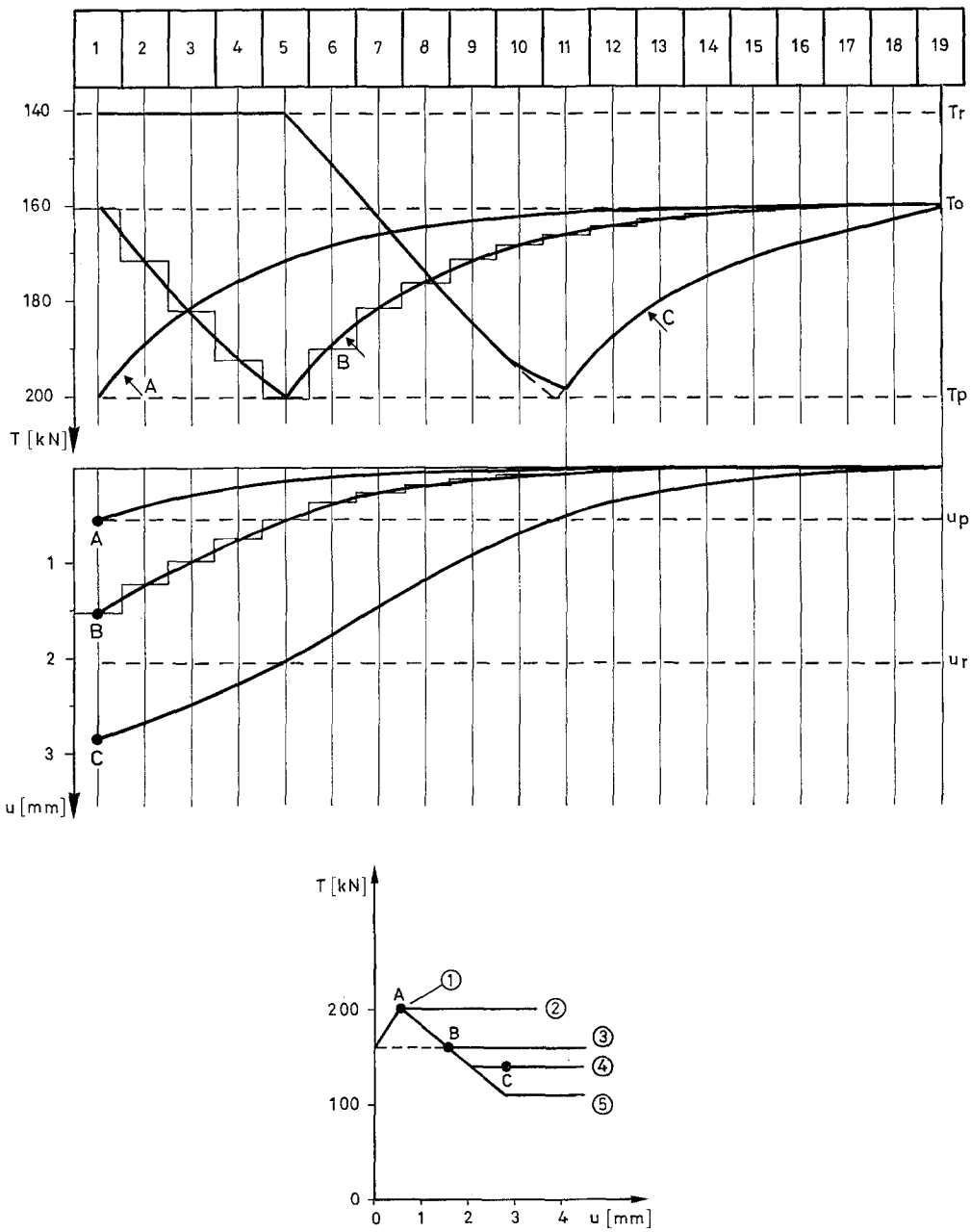

Fig. 7. Progression of failure (shear stress and displacements of blocks)

respond to points A, B, and C in Fig. 6d. The failure is initiated in the first block for a displacement corresponding to point A. Increasing displacements lead to the reduction of shearing resistance under the blocks down to its residual value and the failure advances progressively in the layer.

5. Criterion for Unstable Failure Propagation

The initiation of unstable failure propagation occurs for a critical displacement $u_{1\min}$ corresponding to the minimum support force $Q_{1\min}$. The values of $u_{1\min}$ obtained from support force — displacement curves can be related to shear forces in the shear force displacement relationships. The critical displacement $u_{1\min}$ is practically equal to the displacement u^* (Fig. 5) where the mobilized shear strength is reduced to the value of T_0. It is interesting to notice that this critical displacement depends only on the shear behaviour of the bedding plane (Figs. 6b and 6c) and does not depend on Q_0 and K_n (see Figs. 6a and 6f), where K_n and Q_0 are varied but $u_{1\min}$ remains constant.

From the parametric studies it is evident that the magnitude of $Q_{1\min}$ is influenced by the shear stiffnesses K_s, K_s^* and the lateral force Q_0. Several attempts have been made to establish a relationship between these parameters and $Q_{1\min}$. Fig. 8 shows a relation between two dimensionless ratios $\Delta Q/T_p'$ and $\frac{K_n(K_s+K_s^*)}{K_s K_s^*}$, where

$\Delta Q = Q_0 - Q_{1\min}$ represents the difference between the initial force Q_0 and $Q_{1\min}$.

$T_p' = T_p - T_0$ is the shearing resistance available beyond that required to compensate the component of the weight $T_0 = W \sin\beta$.

$\frac{K_n(K_s+K_s^*)}{K_s K_s^*}$ is the ratio representing parameters describing the deformability of joints.

The points in Fig. 8 are determined from parametric studies and are fitted visually with the heavy curve; the dash-dotted curve shown in Fig. 8 can be expressed analytically as

$$\frac{\Delta Q}{T_p'} = \alpha \tag{11}$$

where $\alpha = \left[\frac{K_n(K_s+K_s^*)}{K_s K_s^*}\right]^{1/2}$

The minimum support force $Q_{1\min}$ can then be obtained from Eq. (11)

$$Q_{1\min} = Q_0 - T_p' \cdot \alpha. \tag{12}$$

The relation (12) can be used to determine the stability of an unsupported slope after excavation. Setting $Q_{1\min} = 0$ in Eq. (12) leads to the following

$$Q_0 = T_p' \cdot \alpha. \tag{13}$$

This expression gives the minimum lateral force Q_0 which would cause unstable failure propagation. The same expression may be written in terms of a safety factor:

$$F_s = \frac{T_p'}{Q_0} \cdot \alpha \tag{14}$$

F_s must be greater than unity for a stable slope.

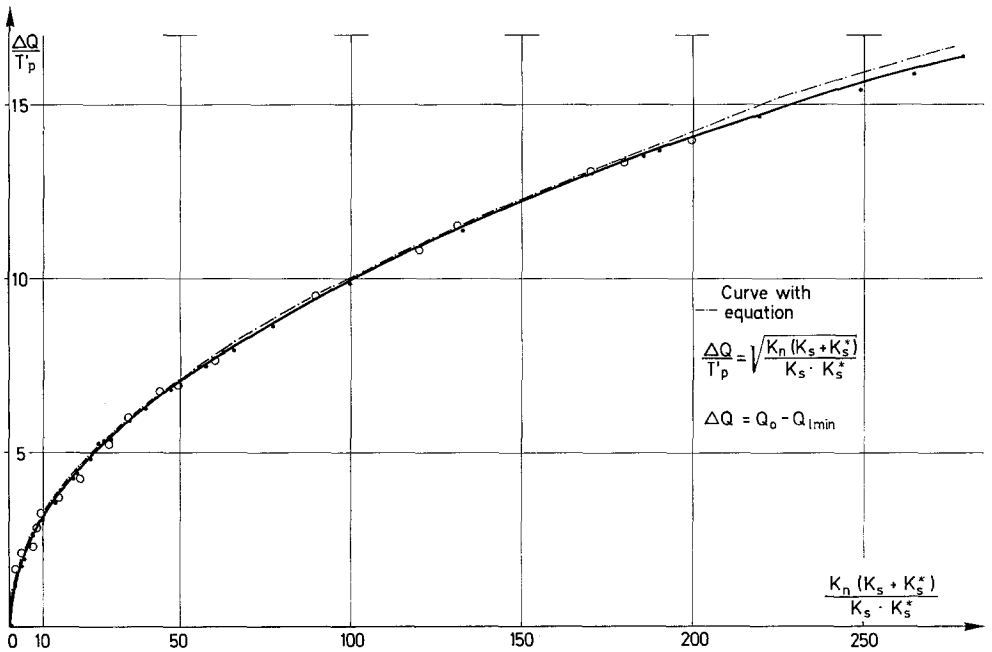

Fig. 8. Relation between bedding surface properties and minimum support force

Eqs. (12) or (14) depend on a number of parameters that need to be determined. Parameters K_s, K_s^*, K_n and T_p can be obtained from shear tests on rock joints. However while T_p, K_s and K_n are usually measured when conducting direct shear tests this is not so for K_s^*. Thus information on K_s^* is not or only to a limited extent available in the literature (Goodman, 1969; Kulhawy, 1975). The determination of the lateral ("Tectonic") force Q_0 is somewhat problematic; stress measurements in situ would have to be conducted, and this often near the surface (Rocha et al., 1966).

Relation (14) for $Q_{1\min}$ can also be obtained by considering the energy balance of the system (Gencer, 1982). The shaded area in Fig. 9a represents the work $J_c - J_g$ done by the shear force over displacement u^*. J_c is the total work due to the shear force and J_g represents the work done by gravity. The quantity of the relevant elastic energy J_q due to the reduction of lateral force Q_0 is shown as a shaded area in Fig. 9b. The latter represents in fact the energy stored in the layer during its geological history. It

is transformed into work performed by the shear force during the movement of blocks.

Equilibrium requires that both quantities must be equal

$$J_c - J_g = J_q. \tag{15}$$

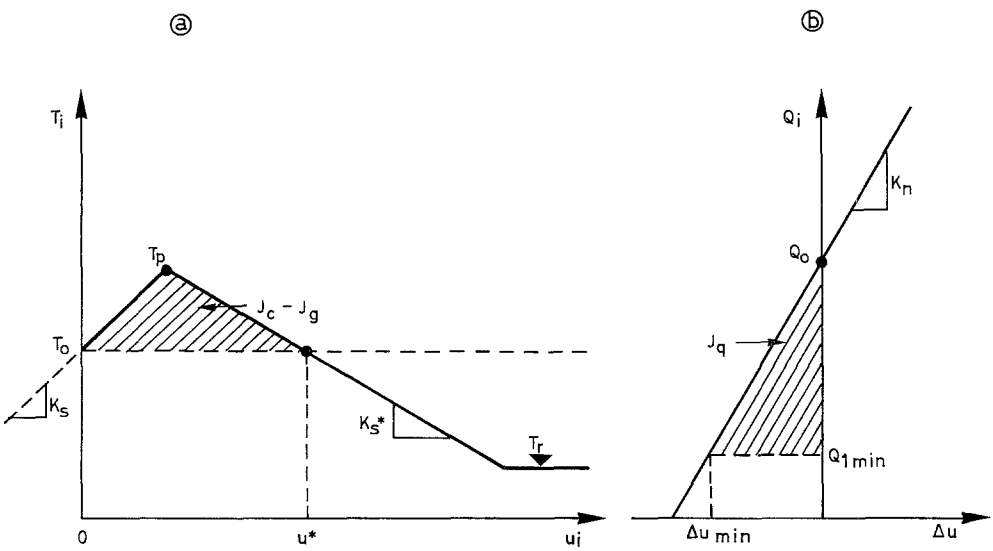

Fig. 9. Determination of the minimum support force with an energy approach

The total stored energy in the layer is given by:

$$J_0 = \frac{Q_0^2}{2K_n}. \tag{16}$$

If J_0 is less than $J_c - J_g$, stored energy is not sufficient to cause initiation of unstable propagation failure.

6. Effect of Time on Progressive Failure

Throughout this presentation the effect of time was neglected. However the reduction of the shearing resistance along the bedding surface is usually a function of both displacement and time.

The actual time dependent behaviour of rock discontinuities is not well understood and a simplified rheological model will be used here.

The forces acting on block i at time t are shown in Fig. 10a. The shear force T_i is assumed to be time dependent while the interblock forces Q_i vary only with displacements (see Eq. 3). The rheological model, shown in Fig. 10b, is a modified form of the Kelvin's viscoelastic model. The shear force T_i has two components. T_s, representing the instantaneous value which depends only on displacement of the block, and T_a which changes

linearly with respect to the velocity of the same block. At time t the shear force T_i is obtained from the equilibrium of a block i.

$$T_i = Q_{i+1} - Q_i - W \sin \beta \tag{17}$$

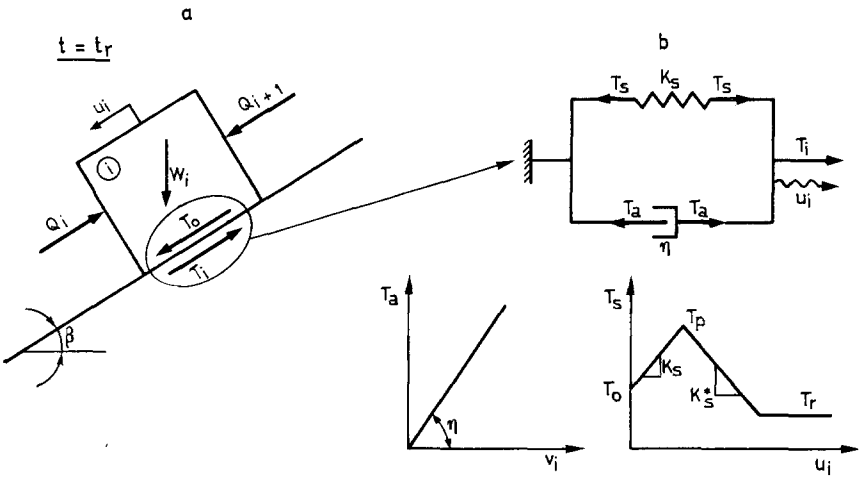

Fig. 10. Time dependent model for shearing behaviour of a rock joint

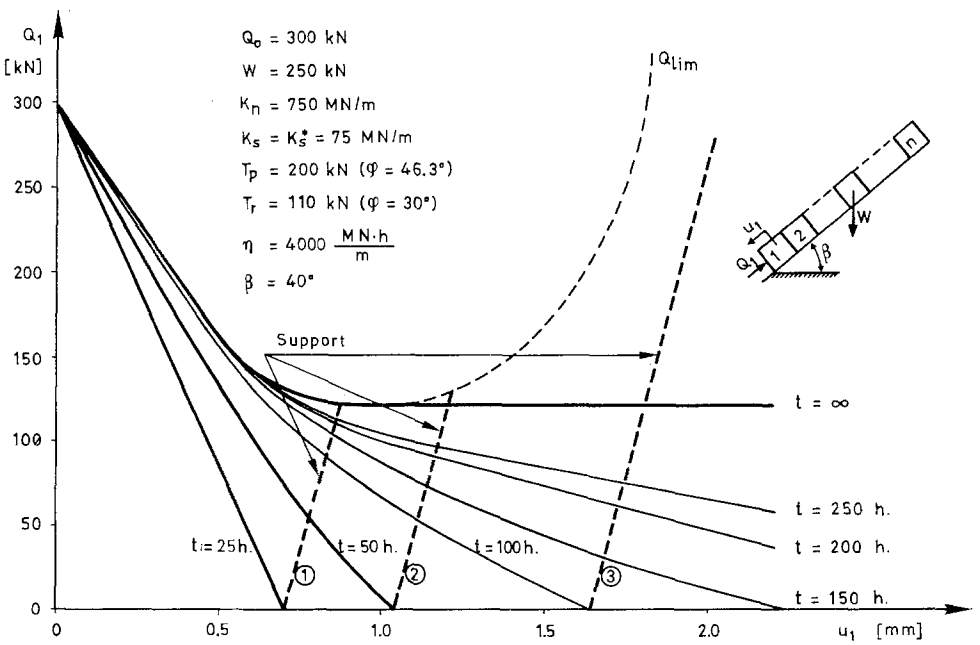

Fig. 11. Variation of the support-force with displacements different amounts of elapsed time (for time dependent shearing resistance)

The value of T_s is computed according to Eqs. (4) and the time dependent component is obtained simply as follows:

$$T_a = T_i - T_s. \tag{18}$$

The velocity of the block is obtained from

$$v_i(t) = \frac{T_a}{\eta} \tag{19}$$

where η is the coefficient of viscosity. The displacement of block i at time $t+\Delta t$ is given by

$$u_i(t+\Delta t) = u_i(t) + v_i(t) \cdot \Delta t \tag{20}$$

where Δt is the time step. Eqs. (17) to (20) are applied to each block by increasing the time steps. As before, the lateral force Q_0 is reduced to a value Q_1 but now the distribution of the forces and displacement can also

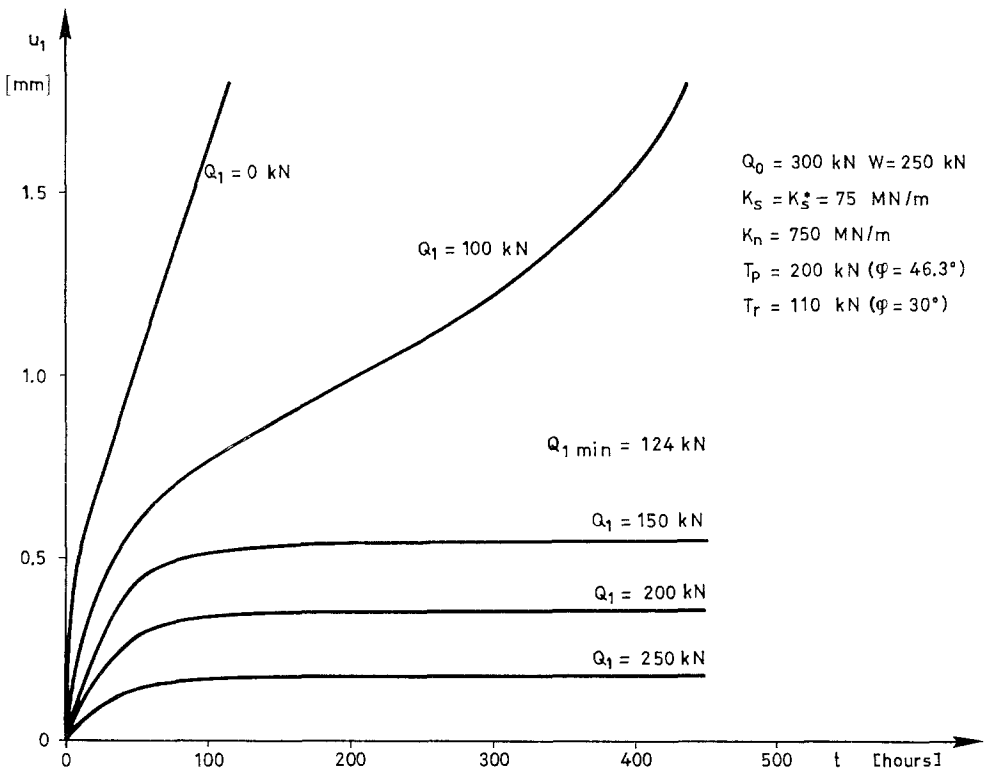

Fig. 12. Time displacement curves for different constant values of applied support pressure Q_1

be obtained with respect to time. The results of an example are presented in Fig. 11. (Q_1 is plotted versus u_1 for different amounts of elapsed time). The displacements increase rapidly with time when the applied force Q_1 is

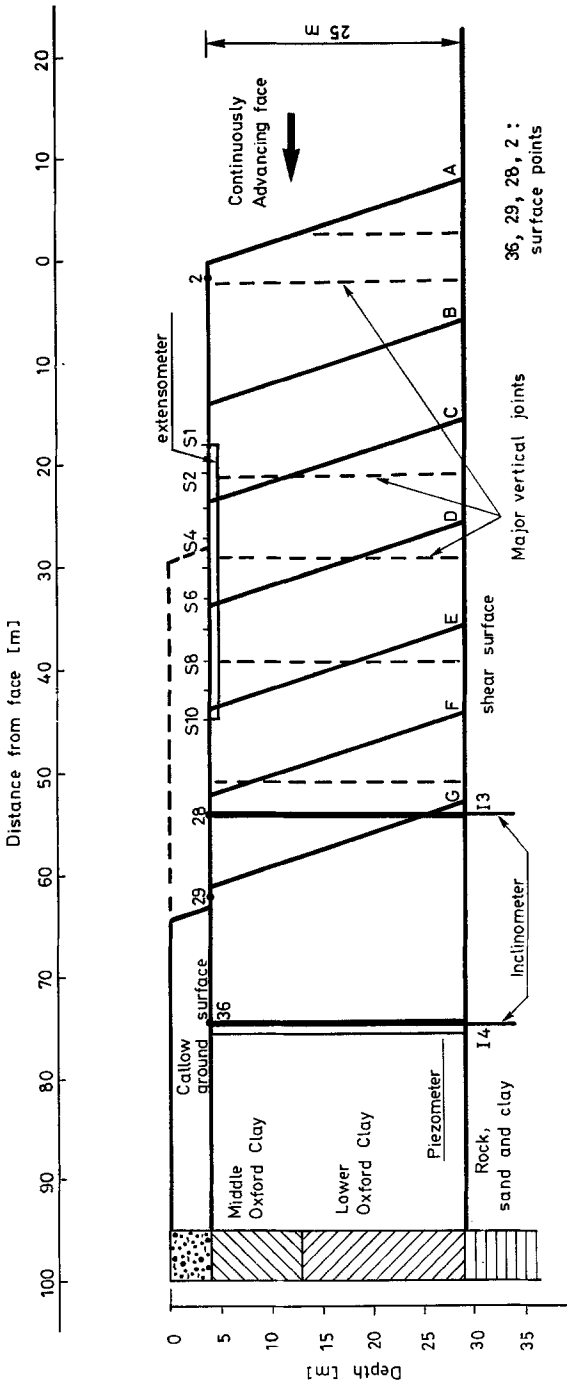

Fig. 13. Case study, center line section normal to the face showing position of successive face, geology and instrumentation (From Burland et al., 1977)

less than the minimum support force $Q_{1\,min}$. For this case tertiary creep like behaviour is reached as illustrated by Fig. 12, which shows the variation of the displacements with time for different values of Q_1. For Q_1 greater than $Q_{1\,min}$ the displacements reach a finite value, while failure occurs for support forces below $Q_{1\,min}$.

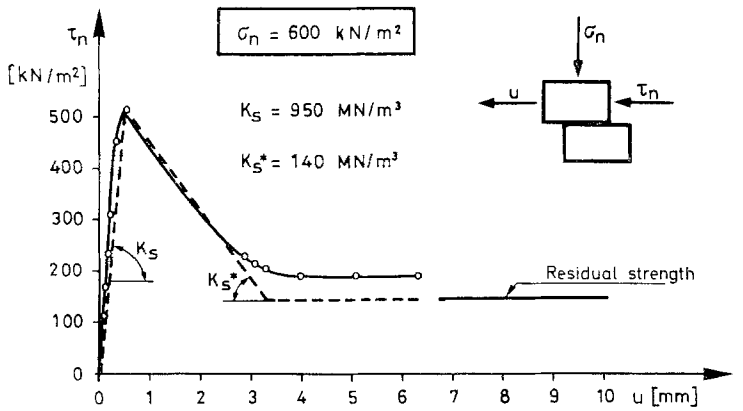

Fig. 14. Typical behaviour of clay sheared parallel to the bedding case study (From Burland et al., 1977)

The time dependent support force-displacement curves in Fig. 11 may be used to determine the optimum time of support application. Assume that the initial force Q_0 is completely removed by excavation and the support is applied after a some amount of elapsed time. The support force will vary in time with increasing displacements at the excavation face. This variation is expressed by the following linear relationship:

$$Q_1 = C\,(u_1 - u_t). \tag{21}$$

where C is the stiffness of the support (e. g. anchor cables), u_t represents the displacement for a given time. This displacement u_t is obtained from the intersection of the time dependent support force-displacement curves (Fig. 11) with the u_1 axis. For example the line 1 in the Fig. 11 represents a support applied after 25 hours. (The slope of that line corresponds to the support stiffness which in this case is taken equal to K_n). The final support force is almost equal to $Q_{1\,min}$. Line 2 represents the same type of support applied after 50 hours. It is still possible to stabilize the excavation, but the final support force is greater than $Q_{1\,min}$ and located in the zone of unstable propagation of failure (The dashed curve represents the time independent support force-displacement curve described previously). Line 3 corresponds again to the same type of support applied too late (no intersection point exists with the time independent $Q_1 - u_1$ relationships). The support force will increase until an eventual rupture occurs in the support.

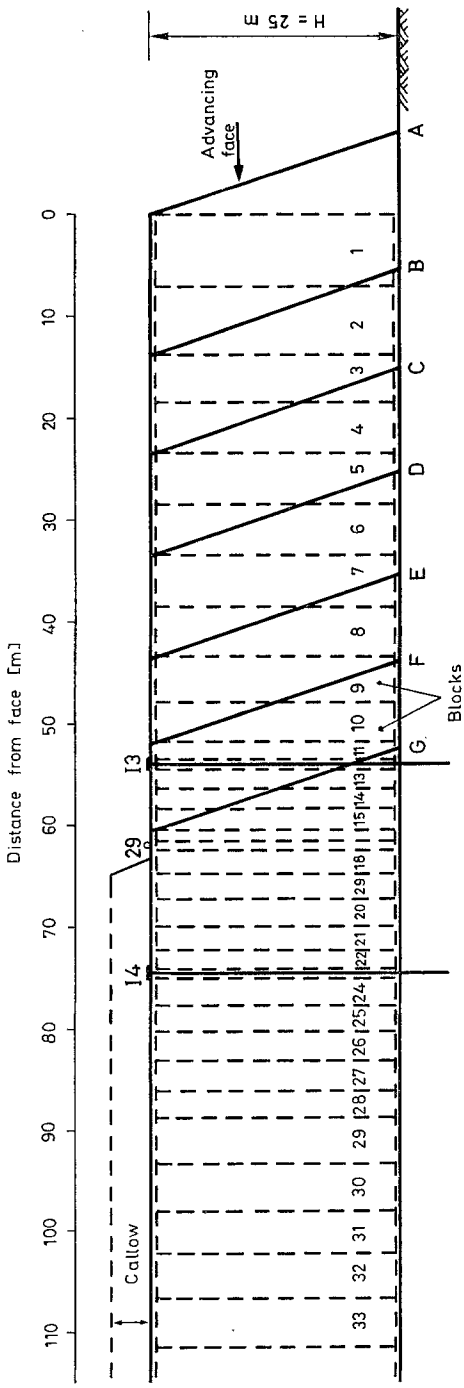

Fig. 15. Case study, Discretisation of the clay mass into blocks

7. Case Study

The progressive failure model was applied to the case study by Burland et al. (1977) which describes an excavation of about 25 m in the highly overconsolidated Oxford Clay at Saxon Pit in England.

The Oxford Clay is horizontally bedded and its most obvious structural features are near vertical major joints. The underlying formation consists of Kelleway Sand and Clay, and limestone (Fig. 13). The process of excavation was carried out in steps *A* to *G* which lead to a stepwise reduction of in situ horizontal stress in the surrounding ground. In each step the clay mass moved as a block, that is the displacements were almost equal at the excavation bottom and at the ground surface. Over thrusting relative to lower beds occurred by sliding along a shear band which developed progressive failure as the maximum shear stress exceeded the peak shear strength along bedding planes near the pit base level. The exceptionally brittle behaviour of intact specimens (taken near the base of the face) when sheared parallel to the bedding, is shown in Fig. 14. (Burland et al., 1977).

Instrumentation was installed to measure displacements both at depth and near the surface. The observed behaviour can be summarized as follows; the release of horizontal stresses at the face of the excavation induces shear stresses some distance away from the face. As the face advances the shear stress at a given location increases until it reaches the peak shear strength along the bedding planes. Relative displacement is then initiated and the shearing resistance drops to a residual value.

To compare the observations with the progressive failure model, the clay mass was discretized into 33 blocks (Fig. 15). The first blocks were removed progressively to simulate the advancing excavation face. Only horizontal displacements are considered since those reflect the dominant behaviour.

Parameters describing the shear behaviour of the bedding planes near the pit base were obtained from the shear tests shown in Fig. 14. However since the horizontal in-situ stress and the horizontal Young's Modulus of the clay mass had not been measured, they had to be estimated:

It is realistic to assume that for such a highly overconsolidated clay the stress ratio K_0 (horizontal stress to vertical stress) is greater than one. On the other hand K_0 should be less than 3.3 corresponding to the value of the passive earth pressure coefficient calculated for average values of effective shearing resistance of clay ($\phi' = 28^0$, $c' = 80\ \mathrm{kN/m^2}$) obtained from drained triaxial tests (Burland et al., 1977). This range of $1 < K_0 < 3.3$ provides an estimate for the in-situ stresses.

A linear relationship between behaviour horizontal stress and displacement is assumed:

$$\sigma_h = \sigma_{h0} - E_h \frac{2\,(u_{i-1} - u_i)}{l_{i-1} + l_i} \tag{22}$$

where u_{i-1}, u_i and l_{i-1}, l_i are the displacements and width of two neighbouring blocks respectively, E_h is horizontal Young's Modulus, σ_{h0} is the

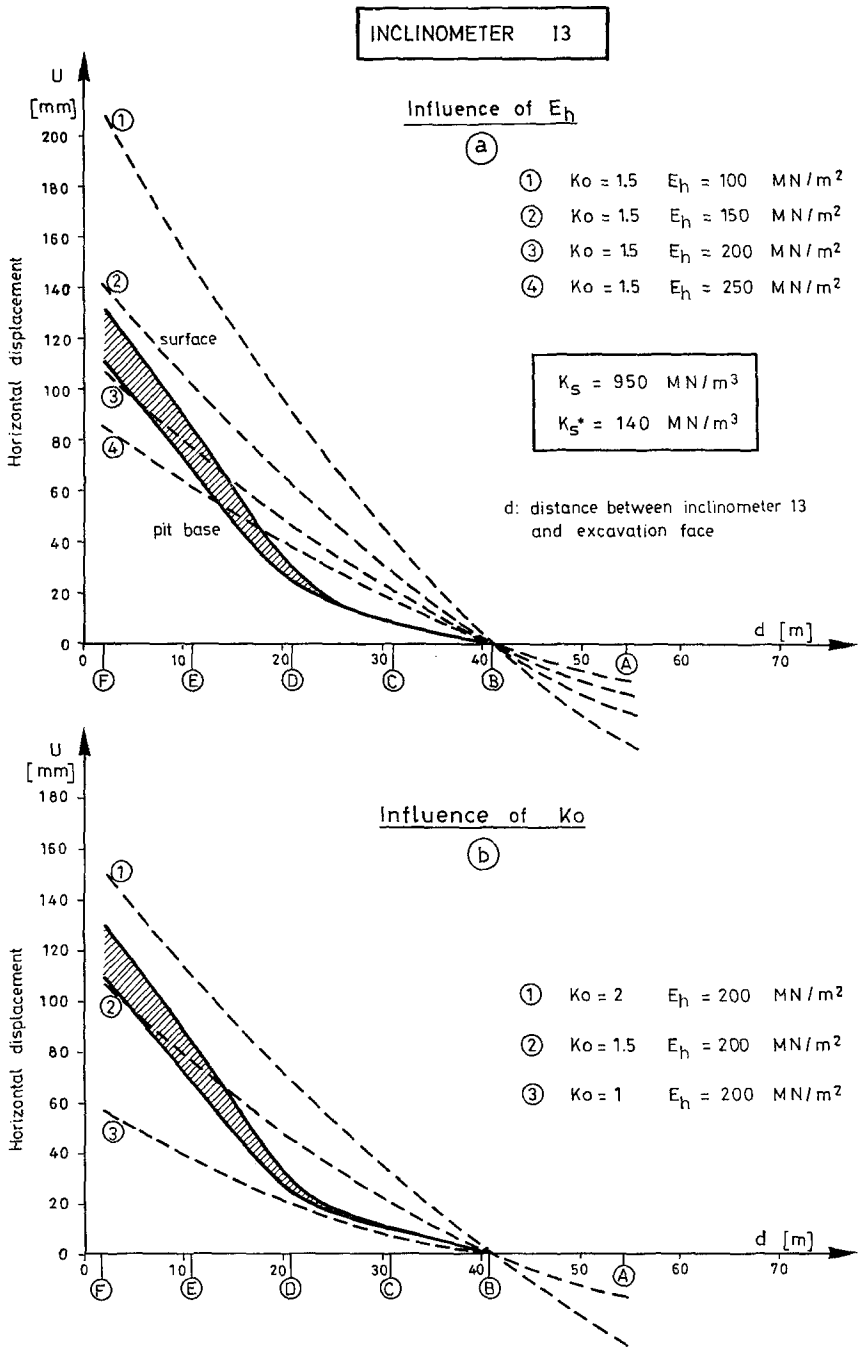

Fig. 16. Comparison of calculated and observed displacements case study

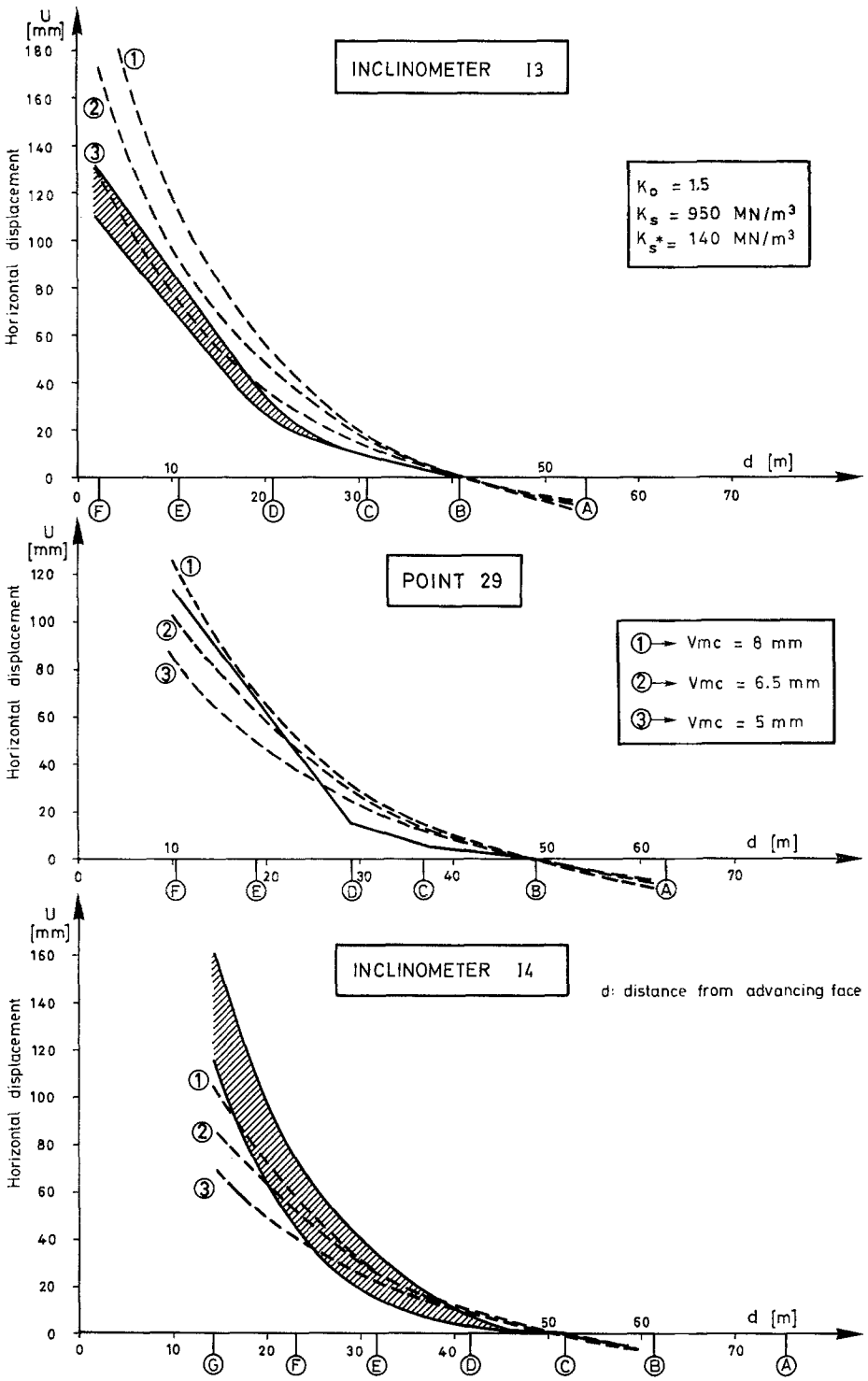

Fig. 17. Comparison of the computed and observed displacements (hyperbolic normal joint deformation)

in-situ horizontal stress before excavation defined as

$$\sigma_{ho} = K_0 \gamma H \tag{23}$$

where γ is the unit weight of soil and H the height of excavation.

In Fig. 16 different values were assumed for the initially unknown parameters K_0 and E_h. The results are compared with the displacements measured by inclinometers I3 and I4 and at surface reference point 29 (see Fig. 15). Fig. 16 shows the comparison of calculated and observed horizontal displacements as a function of distance between inclinometer I3 and the advancing face. The shaded area in Fig. 16 represents the observed displacements at the surface and near the base level. The first results obtained with a constant value of E_h are unsatisfactory. The slope of the curves increase significantly as the distance to I3 becomes smaller. This is probably due to the opening of the major joints which causes a significant reduction of the horizontal Young's Modulus. Thus a hyperbolic relation, as proposed by Goodman (1974), which describes the deformation of the joints with no tensile strength under normal loading, is used to represent the horizontal deformability of the clay mass due to the opening of major joints;

$$\sigma_h = \sigma_{ho} \frac{\Delta u}{v_{mc} - \Delta u} + \sigma_{ho}. \tag{24}$$

Where Δu is the relative displacement between two adjacent blocks and v_{mc} is the maximum closure of the joint. Fig. 17 shows the results obtained for different values for v_{mc}. The joint block model provides a satisfactory representation of the observed behaviour of the excavation.

8. Conclusions

The proposed mathematical model can correctly simulate the mechanism of progressive failure in a stratified and jointed rock mass. Support forces required to ensure stability vary with the displacement at the excavation face.

Unstable failure propagation is initiated for a critical displacement $u_{1\,\min}$ corresponding to a minimum support force. For displacements greater than this critical value the required support force increases until failure occurs in the rock mass.

The critical displacement $u_{1\,\min}$ depends only on the shear force-displacement behaviour of the discontinuities (bedding plane) while the minimum support force depends on the initial state of stress, the stiffness parameters describing the shear behaviour and the normal deformability of joints. An analytical expression for the minimum support force was developed which can be used to evaluate safety against unstable failure propagation. The effect of time on progressive failure can also be included.

A case study showed that the model is adequate. Even though no measured values were available for some parameters there was good agreement between measured and calculated displacements.

Since the model is essentially one dimensional and slope parallel strata have to be assumed a number of further developments are desirable; these

include extension to two dimensions, and considering more complex geometries of stratified and jointed rock masses.

Acknowledgement

The research for this paper was conducted at the Swiss Federal Institute of Technology, Lausanne. The author wishes to acknowledge with thanks the valuable support of Prof. F. Descoeudres. Thanks are also due to Dr. P. Egger for helpful discussions and to Professor H. Einstein who revised the text and made useful suggestions.

Appendix

The integration of the equation of motion with respect to time is carried out for each block as follows:

1) The resultant force $P_i\,(t)$ acting on a block i at time t is derived from the Eq. (5).

2) The damping force $R_i\,(t)$ is calculated by the relation

$$R_i\,(t) = k\,\frac{du_i}{dt} \tag{A1}$$

where k is the damping constant or coefficient of viscosity.

3) The final resultant force to be considered in the equation of motion is defined

$$F_i\,(t) = P_i\,(t) - R_i\,(t). \tag{A2}$$

4) The equation of motion $F_i\,(t) = m\,\frac{d^2 u_i}{dt^2}$ (m is the mass of the block) is integrated by finite difference technique, the velocity v_i and the displacement u_i of the block i at time $t+\Delta t$ are calculated.

$$v_i\,(t+\Delta t) = v_i\,(t) + \frac{F_i\,(t)}{m}\,\Delta t \tag{A3}$$

$$u_i\,(t+\Delta t) = u_i\,(t) + v_i\,(t+\Delta t)\cdot \Delta t \tag{A4}$$

Δt is the time increment.

The calculation cycle 1 to 4 is repeated for all blocks at each time iteration step defined by Δt. The static equilibrium state is reached by increasing the time until the velocities and the resultant forces of all blocks converge to "zero" and their displacements remain unchanged.

The integration parameters Δt and k must be chosen adequately in order to assure the numerical stability, for the case considered in this work the following condition must be held for Δt.

$$\Delta t \leq \sqrt{\frac{m}{K_n}} \tag{A5}$$

where K_n is the normal stiffness modulus. The damping constant k is

chosen as a fraction of the critical damping of a parallel dashpot-spring system

$$k = 2f\sqrt{mK_n} \tag{A6}$$

where f may be chosen between 0.6 and 0.9.

References

Bishop, A. W. (1967): Progressive Failure with Special Reference to the Mechanism Causing Int. Proc. Geot. Conf., Oslo, Vol. *2*, 142—150.

Bjerrum, L. (1967): Progressive Failure in Slopes of Overconsolidated Plastic Clay and Clay Shales. Proc. ASCE *93*, SM *5*, 1—49.

Burland, J. B., Longworth, T. I., Moore, J. F. A. (1977): A Study of Ground Movement and Progressive Failure Caused by a Deep Excavation in Oxford Clay. Geotechnique *27* (no. 4), 557—591.

Christian, J. T., Whitman, R. W. (1969): A One Dimensional Model for Progressive Failure. Proc. 7th Int. Conf. Soil Mech. Found. Eng., Mexico, Vol. *2*, 451—545.

Cundall, P. A. (1971): A Computer Model for Simulating Progressive Large Scale Movements in Blocky Rock Systems. Int. Symp. ISRM, Nancy, Vol. *1*, 2—8.

Descoeudres, F. (1974): Stabilité des versants rocheux en liaison avec les modifications apportées par la construction d'autoroutes. Mémoire CERES No. 47, Juin, Liège.

Descoeudres, F., Gencer, M. (1979): Rupture progressive en versant rocheux stratifié et fissuré. Proc. 4th ISRM Cong., Montreux, Vol. I, 613—619.

Gencer, M. (1982): Rupture progressive en versant rocheux stratifié et fissuré. Thèse de doctorat, Ecole Polytechnique Fédérale de Lausanne, 232.

Goodman, R. E. (1969): The Deformability of Joints. ASTM STP 477, 174—196.

Goodman, R. E. (1974): Les propriétés mécaniques des joints. Proc. 3rd ISRM Congr., Denver, Vol. IA, 127—140.

Kulhawy, F. D. (1975): Stress Deformations Properties of Rock and Rock Discontinuities. Engineering Geology No. *9*, 327—350.

Müller, L. (1966): Der progressive Bruch in geklüfteten Medien. Proc. 1st ISRM Congr., Lisbon, Vol. *1*, 679—686.

Müller, L., Malina, H. (1968): Schubspannungsverteilung im progressiven Bruch. Felsmech. und Ingenieurgeol. *6*, 216—224.

Otter, J. R. H., Cassel, A. C., Hobbs, R. E. (1966): Dynamic Relaxation. Proc. Instn. Civ. Engrs. Vol. *35*, 633—656.

Palmer, A. C., Rice, J. R. (1973): The Growth of Slip Surfaces in the Progressive Failure of Overconsoliated Clay. Proc. Royal Soc. London, A332, 527—548.

Rocha, M., Lopes, J. B., Silva, J. N. (1966): A New Technique for Applying the Method of the Flat Jack in the Determination of Stresses Inside Rock Masses. Proc. 1st ISRM Congr., Lisbon, Vol. *2*, 57—65.

Skempton, A. W. (1964): Long Term Stability of Clay Slopes. Geotechnique *14* (no. 2), 77—102.

Suklje, L. (1971): Progressive Failure of Natural Slopes. University of Ljubljana, Acta Geotechnica *34—36*, 17—23.